Mater. Res. Soc. Symp. Proc. Vol. 1314 © 2011 Materials Research Society
DOI: 10.1557/opl.2011.509

Computational Study of the Electronic Performance of Cross-Plane Superlattice Peltier Devices

Changwook Jeong, Gerhard Klimeck, and Mark Lundstrom
Network for Computational Nanotechnology
Purdue University
West Lafayette, Indiana, USA

ABSTRACT

We use a state-of-the-art non-equilibrium quantum transport simulation code, NEMO-1D, to address the device physics and performance benchmarking of cross-plane superlattice Peltier coolers. Our findings show quantitatively how barriers in cross-plane superlattices degrade the electrical performance, i.e. power factor. The performance of an $In_{0.53}Ga_{0.47}As/In_{0.52}Al_{0.48}As$ cross-plane SL Peltier cooler is lower than that of either a bulk $In_{0.53}Ga_{0.47}As$ or bulk $In_{0.52}Al_{0.48}As$ device, mainly due to quantum mechanical effects. We find that a cross-plane SL device has a Seebeck coefficient vs. conductance tradeoff that is no better than that of a bulk device. The effects of tunneling and phase coherence between multi barriers are examined. It is shown that tunneling, SL contacts, and coherency only produce oscillatory behavior of Seebeck coefficient vs. conductance without a significant gain in PF. The overall TE device performance is, therefore, a compromise between the enhanced Seebeck coefficient and degraded conductance.

INTRODUCTION

The dimensionless figure of merit, $ZT = S^2GT/K$, is the primary material parameter governing the maximum thermoelectric (TE) efficiency. Here T is the temperature, S is the Seebeck coefficient, G is the electrical conductance, and K is the thermal conductance, which is the sum of the electronic contribution, K_e , and the lattice thermal conductance, K_{ph} . Most recent improvements in ZT have been achieved by phonon engineering to reduce the lattice thermal conductivity [1-3]. One way is to use thin film superlattices (SLs), which has led to significant reduction in the lattice thermal conductivity and, therefore, enhanced TE performance [4]. The possibility of enhancing the electronic component (S^2G, power factor: PF) of TE performance by using SL devices has been studied. First quantitative calculations for in-plane direction in SLs were done by Hicks and Dresselhaus in 1993 [5,6] and showed promising results. For cross-plane transport in SL, it has been predicted that energy filtering will lead to significant increases in ZT under a certain condition [7]. A single barrier and multi-layer thermionic refrigeration were proposed [8,9]. Experimentally, researchers have shown the increase in S by filtering out low energy electrons, but a limited increase in power factors due to the decrease in electrical conductivity [10-12].

Although there have been a number of studies, it is still not clear how a SL affects the electronic performance i.e. PF. This work explores the physics of transport in single barrier and multi-barrier (i.e. SL) TE devices using a sophisticated quantum transport model, NEMO-1D[13-15]. A clear understanding of how barriers affect the PF is essential for developing single barrier or multi-barrier TE devices with enhanced PF and is the objective of this paper.

APPROACH

In the linear response regime, the Landauer expressions for electronic transport properties such as G, S, and K_e are expressed as

$$G = \left(\frac{2q^2}{h}\right) I_0 \qquad [1/\Omega] \qquad (1)$$

$$S = \left(-\frac{k_B}{q}\right)\frac{I_1}{I_0} \qquad [\mathrm{V/K}] \qquad (2)$$

$$K_e = \left(\frac{2k_B^2 T}{h}\right)\left\{I_2 - \frac{I_1^{\,2}}{I_0}\right\}, \qquad [\mathrm{W/K}] \qquad (3)$$

where

$$I_j = \int_{-\infty}^{+\infty}\left(\frac{E-E_F}{k_B T_L}\right)^j \overline{T}_e(E)\left(-\frac{\partial f_0}{\partial E}\right)dE \qquad (4)$$

with

$$\overline{T}_e(E) = T_e(E) M_e(E) \qquad (5)$$

being the transmission, and $M_e(E)$ the number of electron conducting modes. In this study, $\overline{T}_e(E)$ is evaluated with the NEMO tool [13-15], which was originally developed to simulate resonant tunneling devices (RTDs) by the non-Equilibrium Green's Function (NEGF) approach, rigorously considering quantum mechanical (QM) reflection and interferences and contacts with a phenomenological energy relaxation model. In this study we assume conductors with $T_e(E) = 1$, i.e. ballistic transport. Quantum mechanical effects like quantum reflections, tunneling, and interferences are included in $M_e(E)$.

An $In_{0.53}Ga_{0.47}As/In_{0.52}Al_{0.48}As$ SL is considered as a model structure, and an effective mass model is used in NEMO. To begin with, we examine the hetero-junction and then a single barrier is studied with varying barrier thickness to evaluate quantitatively the effect of tunneling. Then, the effects of multiple barriers are studied. The effect of multiple barriers include first, the effect of "SL contacts" and second, the effects of phase coherency between SL periods. Sketches of test structures are shown in Fig. 1.

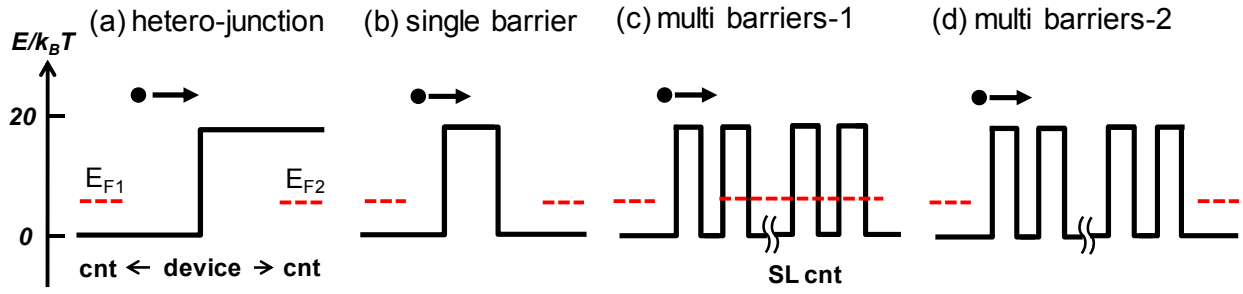

Figure 1. Schematic diagrams of test structure of numerical experiments. (a) hetero-junction, (b) single barrier (c) multi-barriers-1: SL contacts and (d) multi-barriers-2: phase coherency. Barrier is $In_{0.52}Al_{0.48}As$. Grayed box represents contact (cnt), where energy relaxation scattering time is assumed to be 50 fs. Solid circle denotes injected electrons from emitter contact. emitter: bulk $In_{0.53}Ga_{0.47}As$ with 0.044 m_0, barrier: $In_{0.52}Al_{0.48}As$ with 0.075 m_0, barrier height, Φ_B: 0.51 eV.

RESULTS AND DISCUSSION

Hetero-junction and Single barrier

A previous theoretical study [16] suggested a simple general rule in a semiclassical picture that given the transmission (number of conducting modes) in the emitter and the barrier, the smaller one determines overall transmission at the hetero-junction. As shown in Fig. 2(a), the semiclassical transmission (blue solid line) of the hetero-junction is the lower of transmission of bulk $In_{0.53}Ga_{0.47}As$ and that of bulk $In_{0.52}Al_{0.48}As$. For the most of energy range, the overall transmission is determined by the barrier because of its lower number of conducting modes. The NEMO simulations at the hetero-junction were compared to the semiclassical transmission. It is seen that the slope of NEMO $\overline{T}_e(E)$ becomes shallower than semiclassical one due to QM reflection at the junction interface. The inset of Fig. 2(a) is a contour plot of NEMO transmission at hetero-junction as a function of longitudinal energy (horizontal-axis) and transverse energy (vertical-axis). Note that transmission is close to one even when incident longitudinal energy is less than barrier height or close to zero. This occurs because of transverse momentum and total energy conservation condition at the interface. In the case of homo-junction, however, the transmission is independent of the transverse energy which is not shown here. In comparison to the hetero-junction, the transmission for the single barrier with barrier thickness of 20 nm (thick enough to suppress tunneling current) is smaller due to Fabry-Perot type interference. Therefore, it can be easily predicted that QM evaluation of transmission gives worse electrical conductance than semiclassical approach. In addition, the weak energy dependence of transmission produces a small S from Eq. (2). Overall S vs. G tradeoff and PF vs. E_F are shown in Fig. 3(a) and 4(a). It is seen that PF of a single barrier is about 50% of bulk $In_{0.52}Al_{0.48}As$ and no better than hetero-junction and bulk $In_{0.53}Ga_{0.47}As$.

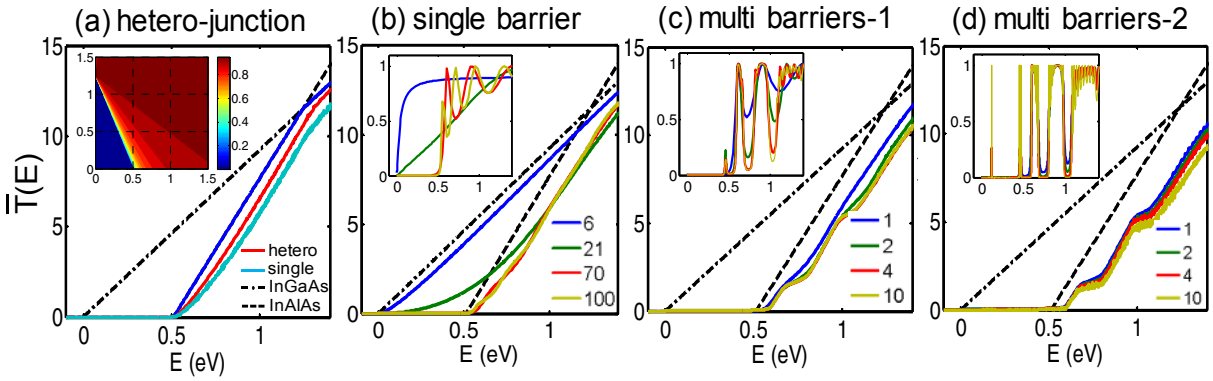

Figure 2. Transmission results: (a) semi-classical (blue) for hetero-junction vs. QM calculation for hetero-junction (red) and single barrier (light blue). Barrier thickness is 200 Å (b) single barrier. Barrier thickness: 6, 21, 70, 100 Å (c) multi-barriers-1 (no. of barriers in SL contacts): 1, 2, 4, 10, and (d) multi-barriers-2 (no. of barriers in device region): 1, 2, 4, 10. The dashed dot is bulk $In_{0.53}Ga_{0.47}As$ and dashed line is $In_{0.52}Al_{0.48}As$. Insets: (a) contour plot of transmission at hetero junction as a function of longitudinal energy (x-axis) and transverse energy (y-axis), (b-d) transmission (y-axis) vs. total energy (x-axis, in *eV*) plot when transverse energy is zero.

Next, the effect of tunneling is quantitatively evaluated in a single barrier. Figure 2(b) shows the transmission for barrier thickness of 6, 21, 70 and 100 Å. As the barrier thickness gets

smaller, i.e., tunneling contribution is dominant, the overall curve is reduced to $\overline{T}_e(E)$ of bulk $In_{0.53}Ga_{0.47}As$ and energy dependency of $\overline{T}_e(E)$ becomes weak. The corresponding results of S vs. G tradeoff and PF vs. barrier thickness are shown in Fig. 3(b) and 4(b). In Fig. 4(b), comparing to thick barrier case (ex: 200 Å), it can be seen that PF generally decreases with thickness down to 21 Å and then increases again to the value of bulk $In_{0.53}Ga_{0.47}As$. However, the behavior of PF from 200 down to 21 Å shows a local maximum of PF at thickness of 70 Å, which is in contrast to the conventional notion that electrons should not tunnel through barriers for maximum cooling performance. The 15% improvement in comparison to thick barrier case is attributed to the delicate interplay between S and G as shown in Fig. 3(b): This behavior results from non-monotonic behavior of S vs. E_F due to non-negligible tunneling current. It can be understood from the two band model: $S_{tot} = (S_1G_1 + S_2G_2)/(G_1 + G_2)$, where $S_1 = -(\Phi_B - E_F + \Delta_{n1})/qT$ and $S_2 = -(-E_F + \Delta_{n2})/qT$ are S of thick barrier ($In_{0.52}Al_{0.48}As$) and bulk emitter ($In_{0.53}Ga_{0.47}As$), respectively and are weighted by thermionic emission over the barrier, G_1 and tunneling current, G_2. Bandstructure and QM effects affect the value of Δ_n. At the fixed $E_F > 0$, it is seen that absolute value of S_1 is larger than S_2. At the barrier thickness of 70 Å, S_{tot} at low E_F is the same as S_2 because high barrier heights ($\Phi_B - E_F$) suppress G_1 and the dominant current is G_2. However, S_{tot} becomes S_1 at high E_F due to $G_1 > G_2$. Transition from small S_2 to large S_1 gives oscillatory behavior of S_{tot} vs. E_F (or S vs. G as shown in Fig. 3(b)). The location of local maximum of S_{tot} depends on barrier thickness: local maximum of S_{tot} vs. E_F moves toward lower E_F as barrier becomes thick. Though this behavior enhances PF slightly, tunneling generally degrades the electronic performance.

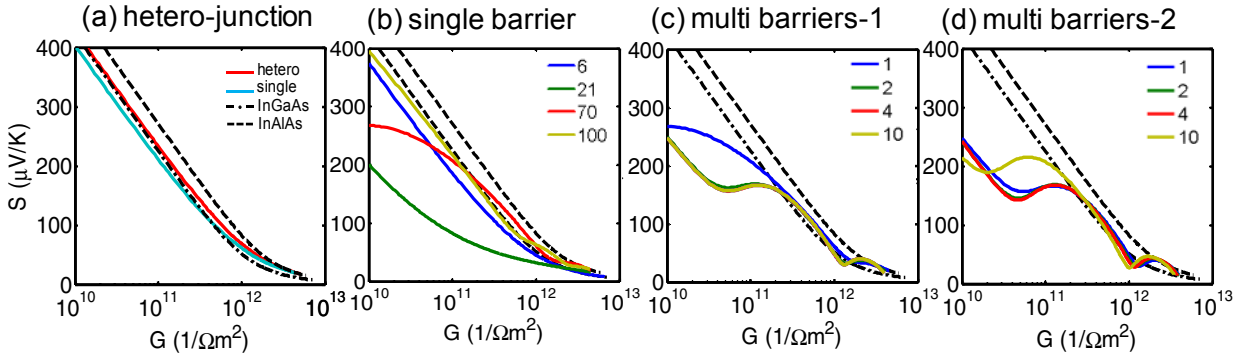

Figure 3. S vs. G trade-off: In each panel, the dashed dot is bulk $In_{0.53}Ga_{0.47}As$; dashed line is $In_{0.52}Al_{0.48}As$. (a) semiclassical results for hetero-junction; red solid line is NEMO calculation for hetero-junction, and light blue line is NEMO calculation for single barrier with barrier thickness of 200 Å (b) single barrier. Barrier thickness: 6, 21, 70, 100 Å (c) multi-barriers-1, no. of barriers in SL cnts + a single barrier device: 1, 2, 4, 10, and (d) multi-barriers-2, no. of barriers in device region: 1, 2, 4, 10.

Multi Barriers

Firstly, the effect of "SL contacts" is studied to see if there is possibility to enhance the PF of a single barrier TE device when it is the first period of SL as shown in Fig. 1(c). A single period of SL is composed of $In_{0.53}Ga_{0.47}As$ (50 Å)/ $In_{0.52}Al_{0.48}As$ (70 Å). As shown in the inset of Fig. 2(c), SL contacts produce mini-bands, though they are not sharply defined because strong

phase relaxation is assumed ($\tau = 5 \times 10^{-14}$ s corresponding to a broadening of 6.6 meV). The effects of SL contacts saturates as the number of periods increase from 2 periods of SLs to 9 periods of SLs in the contact (total no. of barrier is 10). The $\overline{T}_e(E)$ for SL contacts is no better than a single barrier case, resulting in poor PF as shown in Fig. 4(c).

Next, we examine how phase coherency between the SL periods affects the performance. The device region is extended from 1 barrier to 10 barriers. Increasing coherency between SL periods makes more sharply defined mini-bands, resulting in a step-like $\overline{T}_e(E)$ curve, as shown in Fig. 2(d). It is also seen that $\overline{T}_e(E)$ becomes shallow as coherency become stronger. Therefore, this leads to no improvement in PF as shown in Fig. 4(d) though the step shaped $\overline{T}_e(E)$ (or mini-bands) leads to oscillatory *S* behaviors as shown in Fig. 3(c) and (d).

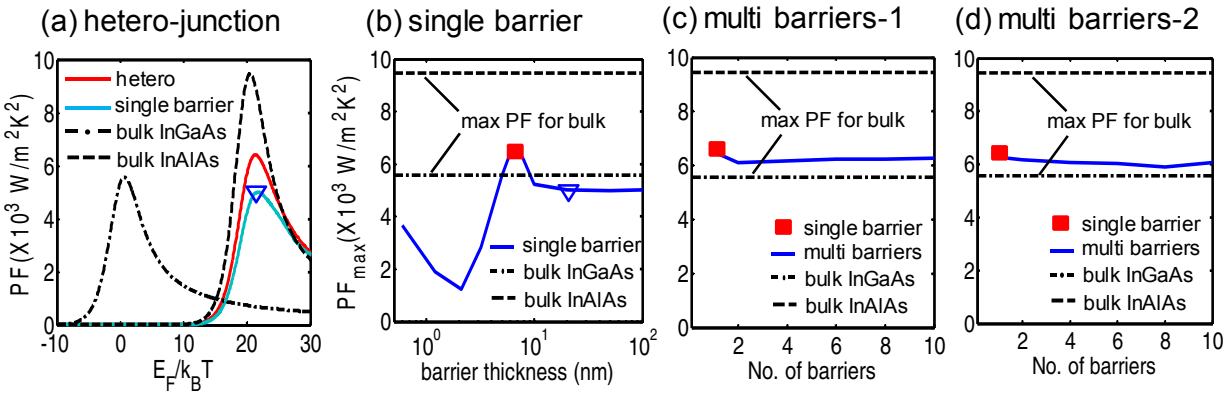

Figure 4. (a) PF vs. E_F results: dashed dot is bulk $In_{0.53}Ga_{0.47}As$, dashed line is $In_{0.52}Al_{0.48}As$ and semi-classical results for hetero-junction, red solid line is NEMO calculation for hetero-junction, and light blue line is NEMO calculation for single barrier with barrier thickness of 200 Å (b) maximum PF (PF_{max}) of single barrier with respect to barrier thickness: 6, 21, 70, 100 Å (c) PF_{max} of multi barriers-1, no. of barriers in SL cnts + a single barrier device: 1, 2, 4, 10, and (d) PF_{max} of multi barriers-2, no. of barriers in device region: 1, 2, 4, 10. The square symbols in (c) and (d) denote PF_{max} of the corresponding single barrier device in (b).

CONCLUSIONS

We examined Peltier cooling in semiconductor SL devices. Quantum transport simulations for hetero-junction and single barrier show that transmission degrades due to QM effects, leading to 50% reduction in PF comparing to bulk barrier materials. In addition, the role of SL contacts and phase coherence in the SL are studied in multi barriers. Our study shows that PF of multi barrier structures is no better than a single barrier TE device. Tunneling, SL contacts and coherency produce oscillatory behavior in the *S* vs. *G* tradeoff, in contrast to conventional monotonic decreasing behavior, but we found no gain in PF. The effect of electrostatic self-consistency, scattering, and SL structure design are under study.

ACKNOWLEDGEMENTS

This work was supported by the Focus Center Research Program (FCRP-MSD). Computational resources were provided by the Network for Computational Nanotechnology (National Science

Foundation under Cooperative Agreement No. EEC-0634750). C. J thanks S. Datta, R. Kim, and S. Shuaib for insightful discussions.

REFERENCES

[1] A. Majumdar, "MATERIALS SCIENCE: Enhanced: Thermoelectricity in Semiconductor Nanostructures," *Science*, vol. 303, Feb. 2004, pp. 777-778.

[2] G.J. Snyder and E.S. Toberer, "Complex thermoelectric materials," *Nat Mater*, vol. 7, Feb. 2008, pp. 105-114.

[3] G. Chen, M.S. Dresselhaus, G. Dresselhaus, J.P. Fleurial, and T. Caillat, "Recent developments in thermoelectric materials," *International Materials Reviews*, vol. 48, 2003, p. 45.

[4] R. Venkatasubramanian, E. Siivola, T. Colpitts, and B. O'Quinn, "Thin-film thermoelectric devices with high room-temperature figures of merit," *Nature*, vol. 413, Oct. 2001, pp. 597-602.

[5] L.D. Hicks, T.C. Harman, and M.S. Dresselhaus, "Use of quantum-well superlattices to obtain a high figure of merit from nonconventional thermoelectric materials," *Applied Physics Letters*, vol. 63, Dec. 1993, pp. 3230-3232.

[6] L.D. Hicks and M.S. Dresselhaus, "Effect of quantum-well structures on the thermoelectric figure of merit," *Physical Review B*, vol. 47, May. 1993, p. 12727.

[7] L.W. Whitlow and T. Hirano, "Superlattice applications to thermoelectricity," *Journal of Applied Physics*, vol. 78, 1995, p. 5460.

[8] G.D. Mahan and L.M. Woods, "Multilayer Thermionic Refrigeration," *Physical Review Letters*, vol. 80, May. 1998, p. 4016.

[9] A. Shakouri, C. LaBounty, J. Piprek, P. Abraham, and J.E. Bowers, "Thermionic emission cooling in single barrier heterostructures," *Applied Physics Letters*, vol. 74, 1999, p. 88.

[10] W. Kim, J. Zide, A. Gossard, D. Klenov, S. Stemmer, A. Shakouri, and A. Majumdar, "Thermal Conductivity Reduction and Thermoelectric Figure of Merit Increase by Embedding Nanoparticles in Crystalline Semiconductors," *Physical Review Letters*, vol. 96, Feb. 2006, p. 045901.

[11] J. Zide, D. Vashaee, Z.X. Bian, G. Zeng, J.E. Bowers, A. Shakouri, and A.C. Gossard, "Demonstration of electron filtering to increase the Seebeck coefficient in $In_{0.53}Ga_{0.47}As/In_{0.53}Ga_{0.28}Al_{0.19}As$ superlattices," *Physical Review B*, vol. 74, Nov. 2006, pp. 205335-5.

[12] J.P. Heremans, C.M. Thrush, and D.T. Morelli, "Thermopower enhancement in lead telluride nanostructures," *Physical Review B*, vol. 70, 2004, p. 115334.

[13] G. Klimeck, R. Lake, R.C. Bowen, W.R. Frensley, and T.S. Moise, "Quantum device simulation with a generalized tunneling formula," *Applied Physics Letters*, vol. 67, 1995, pp. 2539-2541.

[14] G. Klimeck, R. Lake, R.C. Bowen, W.R. Frensley, and D. Blanks, "Nano electronic modelling (NEMO)," *Device Research Conference, 1995. Digest. 1995 53rd Annual*, IEEE, 2002, pp. 52-53.

[15] G. Klimeck, "NEMO 1-D: the first NEGF-based TCAD tool," *Simulation of semiconductor processes and devices 2004: SISPAD 2004*, 2004, p. 9.

[16] R. Kim, C. Jeong, and M.S. Lundstrom, "On momentum conservation and thermionic emission cooling," *Journal of Applied Physics*, vol. 107, 2010, p. 054502.